MAJOR ARTICLE

Mycobacterium tuberculosis Invasion and Traversal across an In Vitro Human Blood-Brain Barrier as a Pathogenic Mechanism for Central Nervous System Tuberculosis

Sanjay K. Jain,[1,2] Maneesh Paul-Satyaseela,[1] Gyanu Lamichhane,[2] Kwang S. Kim,[1] and William R. Bishai[2]

[1]Division of Pediatric Infectious Diseases and [2]Center for Tuberculosis Research, Johns Hopkins University School of Medicine, Baltimore, Maryland

Background. Central nervous system (CNS) tuberculosis is a serious, often fatal disease that disproportionately affects young children. It is thought to develop when *Mycobacterium tuberculosis* breaches the blood-brain barrier (BBB), which is composed of tightly apposed brain microvascular endothelial cells. However, the mechanism(s) involved in this process are poorly understood.

Methods To better understand these processes, we developed an in vitro model of *M. tuberculosis* BBB infection using primary human brain microvascular endothelial cells.

Results. *M. tuberculosis* was found to both invade and traverse the model BBB significantly more than did *M. smegmatis* (a nonpathogenic mycobacterium). Invasion by *M. tuberculosis* across the BBB required host-cell actin cytoskeletal rearrangements. By microarray expression profiling, we found 33 *M. tuberculosis* genes to be highly up-regulated during the early stages of invasion of the BBB by *M. tuberculosis;* 18 of them belong to a previously described in vivo–expressed genomic island *(Rv0960–Rv1001)*. Defined *M. tuberculosis* isogenic transposon mutants for the up-regulated genes *Rv0980c*, *Rv0987*, *Rv0989c*, and *Rv1801* were found to be deficient in their ability to invade the BBB model.

Conclusions. We developed an in vitro model of *M. tuberculosis* BBB infection and identified *M. tuberculosis* genes that may be involved in CNS invasion.

Tuberculosis infects 1.3 million new patients and causes 450,000 deaths among children annually [1]. Tuberculosis of the central nervous system (CNS) is a serious, often fatal disease that disproportionately affects young children [2–5]. CNS tuberculosis is difficult to diagnose and treat; treatment includes 4 drugs that prevent death or disability in fewer than one-half of patients [4–6].

The CNS is protected by the physiological blood-brain barrier (BBB), which is composed of tightly apposed brain microvascular endothelial cells held together by tight junctional complexes [7]. CNS tuberculosis is believed to develop when *Mycobacterium tuberculosis* breaches this barrier, which leads to the development of parenchymal (cortical) and meningeal tuberculomas [8–13]. Tuberculous meningitis may further develop when mycobacteria are released into the subarachnoid space because of caseation of these tuberculomas [9, 14]. It is clear that *M. tuberculosis* invades the CNS, but the host and microbial mechanism(s) involved in this process are poorly understood. Theoretically, *M. tuberculosis* may cross the BBB as free (extracellular) organisms or via infected monocytes/neutrophils. Although the latter hypothesis seems attractive, such cellular traffic is severely restricted into

Received 17 September 2005; accepted 16 November 2005; electronically published 28 March 2006.

Presented in part: Tuberculosis: Integrating Host and Pathogen Biology (D1), Keystone Symposia, Whistler, Canada, 2–7 April 2005 (poster 2030); Pediatric Academic Societies Annual Meeting, Washington, DC, 14–17 May 2005 (poster 1391); Infectious Diseases Society of America Conference, San Francisco, CA, 12–15 October 2005 (abstract 51 and poster 188).

Potential conflicts of interest: none reported.

Financial support: Eudowood Foundation (Baurenschmidt Postdoctoral Research Fellowship to S.K.J.); National Institutes of Health (grants/contracts AI47225 and NS26310 to K.S.K. and AI36973, AI37856, AI43846, AI51668, and AI30036 to W.R.B.).

Reprints or correspondence: Dr. William R. Bishai, Center for Tuberculosis Research, 1550 Orleans St., Baltimore, MD 21231 (wbishai@jhmi.edu).

The Journal of Infectious Diseases 2006;193:1287–95

0022-1899/2006/19309-0015$15.00

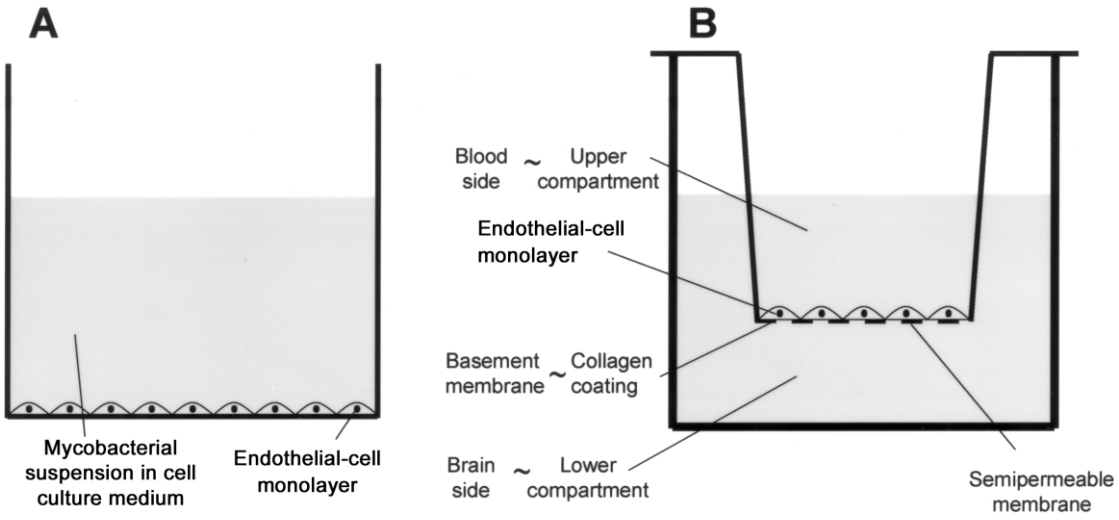

Figure 1. *A,* Invasion assay. A confluent infant human brain microvascular endothelial-cell (HBMEC) monolayer in 24-well plates was infected with a mycobacterial suspension. The plate was centrifuged, incubated for 90 min, washed to remove extracellular mycobacteria, incubated with amikacin for 2 h to kill the remaining extracellular mycobacteria, washed again, lysed, and finally plated to determine the no. of intracellular mycobacteria. *B,* Traversal assay. The polarized in vitro model was formed by growing infant HBMECs to confluence as a monolayer on transwell inserts. Separate access was provided for the upper (blood side) and lower (brain side) compartments. The monolayer was infected by the addition of a mycobacterial suspension to the upper compartment and incubated for 48 h. After 48 h, the contents of the lower compartment were removed and plated to determine the number of mycobacteria that traversed the monolayer (adapted from [25]).

the CNS before invasion by an offending pathogen [15, 16]. Intravenous inoculation of free *M. tuberculosis* in guinea pigs and *M. bovis* in rabbits has been shown to produce CNS invasion, as evidenced by the formation of tuberculomas in their brain parenchyma [8–10]. Experiments in $CD18^{-/-}$ knockout mice have shown that free mycobacteria enter the CNS hematogenously and that monocytes/neutrophils may not be required for this transport [17]. In vitro studies have demonstrated that free *M. tuberculosis* invades endothelial cells [18, 19], and evidence from human autopsy samples supports this concept [20].

Few in vitro or in vivo models are available to study CNS invasion by *M. tuberculosis*. An in vitro model using human brain microvascular endothelial cells (HBMECs) has been used to determine the mechanisms of CNS invasion by other meningitis-causing organisms [21]. We adapted this model for the study of host and microbial factors associated with CNS tuberculosis.

MATERIALS AND METHODS

Cell-culture media. HBMECs were grown in RPMI 1640 medium (Cambrex BioScience) supplemented with 10% heat inactivated fetal bovine serum (FBS; Omega Scientific), 10% Nu Serum (BD Biosciences), L-glutamine (Irvine Scientific), sodium pyruvate, MEM nonessential amino acids, and MEM vitamins (both Cellgro Mediatech). HBMEC experiments were performed using experimental medium that contained 1:1 Ham's F12: medium 199 (Invitrogen) supplemented with 5% heat-inactivated FBS and L-glutamine. HBMEC monolayers were washed using 1:1 Ham's F12: medium 199 with L-glutamine.

M. tuberculosis *strains and media.* *M. tuberculosis* H37Rv, *M. tuberculosis* CDC 1551, *M. bovis* bacille Calmette-Guérin (BCG; Pasteur strain), and *M. smegmatis* were grown to the log phase in plastic roller bottles or as shaken cultures in plastic tubes at 37°C in Middlebrook 7H9 liquid broth (Difco Laboratories) supplemented with oleic acid albumin dextrose catalase (Becton Dickinson), 0.5% glycerol, and 0.05% Tween 80. Colony-forming unit counts were determined by plating mycobacteria onto Middlebrook 7H10 medium (Difco Laboratories). Before the inoculation of HBMECs, all mycobacteria were washed and resuspended in experimental medium at 37°C, and their optical densities at 600 nm were adjusted to achieve the required MOI. In addition, 100 μL from each inoculum was plated to determine the colony-forming unit counts. For the traversal assays, colony-forming unit counts for the infected medium from the upper compartment was also determined at 48 h, to adjust for any mycobacterial replication.

In vitro model of the human BBB with HBMECs. Primary HBMECs were isolated, characterized, and purified from the cerebral cortex of a 9-month-old infant, as described elsewhere [22–24]. This process was exempt from institutional review board approval. The in vitro monolayer was created by cultivating HBMECs on collagen-coated wells of a 24-well plate or in semipermeable (5 μm pore size) transwell polycarbonate tissue culture inserts (Costar) (figure 1). The HBMEC mono-

Table 1. Genes up-regulated by at least 8-fold in human brain microvascular endothelial-cell–associated vs. –unassociated *Mycobacterium tuberculosis* H37Rv.

H37Rv gene no.	Gene name	Fold change	*P*	Function/probable function
Rv0368c		10.42	.0002	Conserved hypothetical protein
Rv0573c		9.10	.0002	Conserved hypothetical protein
Rv0619	*galTb*	9.90	.0002	Galactose-1-phosphate uridylyl transferase
Rv0661c		9.45	.0002	Conserved hypothetical protein
Rv0662c		8.24	.0006	Conserved hypothetical protein
Rv0966c		18.40	.0001	Conserved hypothetical protein
Rv0967		8.16	.0003	Conserved hypothetical protein
Rv0968		17.02	.0001	Conserved hypothetical protein
Rv0970		9.59	.0002	Conserved integral membrane protein
Rv0971c	*echA7*	8.09	.0002	Enoyl-CoA hydratase
Rv0974c	*accD2*	9.08	.0002	Fatty-acid metabolism
Rv0975c	*fadE13*	8.59	.0002	Lipid degradation
Rv0977	*PE-PGRS16*	10.44	.0002	PE-PGRS family protein
Rv0978c	*PE-PGRS17*	12.86	.0002	PE-PGRS family protein
Rv0980c	*PE-PGRS18*	10.27	.0002	PE-PGRS family protein
Rv0982	*mprB*	8.97	.0002	Two-component sensor kinase
Rv0983	*pepD*	18.28	.0001	Serine protease
Rv0984	*moaB2*	12.01	.0002	Molybdopterin biosynthesis
Rv0986		23.04	.0001	Active transport of adhesion component across membrane, energy coupling to the transport system
Rv0987		10.79	.0002	Active transport of adhesion component across membrane, translocation of the substrate across the membrane
Rv0989c	*qrcC2*	8.43	.0002	Supplier of polprenyl diphosphate
Rv0990c		9.52	.0002	Hypothetical protein
Rv0991c		10.44	.0002	Serine-rich protein
Rv1726		8.54	.0002	Oxireductase
Rv1801	*PPE29*	9.16	.0002	PPE family protein
Rv1966	*mce3A*	8.56	.0003	Involved in host-cell invasion
Rv1968	*mce3C*	19.95	.0001	Involved in host-cell invasion
Rv2318	*uspC*	8.14	.0003	Involved with active transport of sugars across the cell membrane
Rv3021c	*PPE47*	8.74	.0002	PPE family protein
Rv3349c		11.92	.0002	Transposase
Rv3351c		10.43	.0002	Conserved hypothetical protein
Rv3639c		8.22	.0003	Conserved hypothetical protein
Rv3833		9.18	.0002	Transcription regulatory protein

NOTE. Shaded genes belong to a recently described in vivo–expressed genomic island; genes in bold type are predicted to be nonessential for in vitro growth. CoA, coenzyme A; PE, amino acids Pro-Glu; PGRS, polymorphic GC-rich repetitive sequences; PPE, amino acids Pro-Pro-Glu.

layer on collagen-coated transwell inserts exhibits tight junction formation and polarization and develops high transendothelial electrical resistance (TEER; 300–600 Ω/cm^2) [22–24]. Culture medium was changed every 2 days, and confluence was determined by light microscopy or by measuring TEER using a Millicell-ERS apparatus (World Precision Instruments).

Invasion assay. A total of 100,000 HBMECs/well were seeded and were confluent on days 3–4 (500,000 cells/well). This monolayer was infected with the mycobacterial suspension (MOI, 10–50), centrifuged (at 890 *g* for 10 min), and incubated for 90 min at 37°C in 5% CO_2. The monolayer was washed, to remove the extracellular mycobacteria, and incubated with 200 μg/mL amikacin for 2 h at 37°C in 5% CO_2, to kill any remaining extracellular mycobacteria [18]. Our preliminary experiments showed that, under the conditions used in our assay, incubation of mycobacteria with 200 μg/mL amikacin for 2 h achieves 99% killing. The monolayer was washed again and lysed using sterile water, and colony-forming unit counts were determined for the quantification of intracellular mycobacteria. Invasion was expressed as a percentage of the inoculum.

Traversal assay. A total of 20,000 HBMECs/transwell were seeded and were confluent by day 8 (200,000 HBMECs/transwell). The monolayer was infected by inoculating the mycobacterial suspension (MOI, 10–50) in the upper compartment. The transwells were then incubated for 48 h at 37°C in 5% CO_2. Thereafter, all contents of the lower compartment (~1 mL) were plated for colony-forming unit counts for quantification of the mycobacteria that traversed the monolayer. Traversal was expressed as a percentage of the inoculum.

Visualization by transmission electron microscopy of* M. tuberculosis *interaction with HBMECs. At the end of 48 h, infected transwells from the traversal assay were washed several times and fixed overnight with ice-cold 100 mmol/L cacodylate buffer that contained 3% formaldehyde, 1.5% glutaraldehyde, and 5 mmol/L $CaCl_2$ (pH, 7.4). The monolayers were postfixed in Palade's OsO_4, stained en bloc in Kellenberger's uranyl ac-

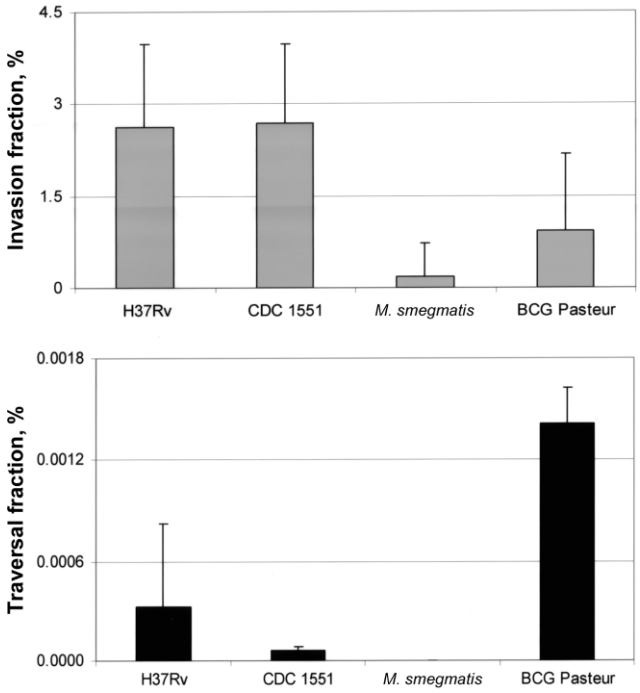

Figure 2. Invasion *(top)* and traversal *(bottom)* of the infant human brain microvascular endothelial-cell (HBMEC) monolayer by different species of mycobacteria. *Mycobacterium tuberculosis* (strain H37Rv or CDC1551) invades and traverses HBMECs at significantly higher rates than does *M. smegmatis* ($P < .01$). Invasion and traversal by *M. bovis* bacille Calmette-Guérin (BCG) was not significantly different from that for *M. tuberculosis* ($P > .06$). Medians are shown; the error bar represents the third quartile. Groups were compared statistically using the Mann-Whitney *U* test.

etate, dehydrated through a graded alcohol series, and embedded in Spurr resin. Ultrathin sections were cut with a Leica UCT ultramicrotome and were viewed with a Philips EM 420 transmission electron microscope. Images were recorded using the Soft Imaging system.

Colocalization of* M. tuberculosis *with HBMEC actin. HBMECs were grown to confluence on collagen-coated glass coverslips in 24-well plates, as described above. They were infected with a suspension of green fluorescent protein (GFP) expressing *M. tuberculosis* CDC 1551 (MOI, ~40) and incubated for 4 h at 37°C in 5% CO_2. The wells were then washed several times, fixed with fresh 4% paraformaldehyde, permeablized with 0.1% Triton X-100, and stained with 1:100 Alexa Fluor 568 phalloidin (Molecular Probes). The coverslips were mounted onto slides, and several fields were visualized using the Zeiss 410 confocal microscope. Image J (version 1.32i; National Institutes of Health) with the Volume J plug-in was used for image reconstruction.

Inhibition assay with cytochalasin D. Cytochalasin D (Calbiochem) was dissolved in dimethyl sulfoxide to make a 10-mmol/L stock solution that was diluted in experimental medium to 0.05 and 0.25 μg/mL. HBMECs were grown to confluence and treated with experimental medium with and without cytochalasin D 1 h before the start of the experiment. The monolayer was infected with *M. tuberculosis* H37Rv (MOI, ~40), and the invasion assay was performed as described above. The integrity of the HBMEC monolayer was inspected several times during the experiment and before lysis of the monolayer.

M. tuberculosis *genes involved in invasion and intracellular survival in HBMECs.* To identify potential *M. tuberculosis* genes involved in invasion and intracellular survival in HBMECs, we studied the *M. tuberculosis* gene-expression profile after interaction with these specialized endothelial cells. mRNA was extracted from *M. tuberculosis* organisms that were HBMEC-associated (either internalized or tightly adherent) and HBMEC-unassociated (nonadherent) during the early stage of invasion. HBMECs were grown to confluence in 2 collagen-coated 150-mm tissue-culture plates for each experiment. The *M. tuberculosis* H37Rv suspension was inoculated on the HBMECs (MOI, ~40) and incubated for 2 h at 37°C in 5% CO_2. Thereafter, the supernatant with unassociated mycobacteria was removed and saved. The HBMEC monolayer was washed several times, to remove nonadherent extracellular mycobacteria, and then lysed with 5 mol/L guanidine isothiocyanate lysis buffer [26]. *M. tuberculosis* H37Rv was recovered by centrifugation at 1335 *g*, and RNA was extracted from both HBMEC-associated and -unassociated *M. tuberculosis* H37Rv using standard methods [27]. Total bacterial RNA extracted from both HBMEC-associated and -unassociated *M. tuberculosis* H37Rv was treated with DNase, to remove contaminating DNA. These were used to prepare cDNA using the Atlas Fluorescent Labeling Kit (BD Biosciences) and were labeled with Cy3 and Cy5 monofluorescent dyes (Amersham Pharmacia). Equal amounts of Cy5-labeled cDNA, prepared using RNA from HBMEC-unassociated *M. tuberculosis* H37Rv, and Cy3-labeled cDNA, prepared using RNA from HBMEC-associated *M. tuberculosis* H37Rv, were cohybridized onto a printed oligonucleotide microarray representing all open reading frames (ORFs) of *M. tuberculosis* (Operon Biotechnologies). The arrays were scanned using the GenePix Scanner 4000B (Axon Instruments). Five different sets of mRNAs prepared from 5 independent experiments were analyzed, to minimize experimental artifacts and microarray-associated systematic errors. Fluorescence intensities obtained from microarrays were normalized. Significance Analysis of Microarrays software (version 1.21; Stanford University) was used to identify genes that were significantly differentially regulated by at least 8-fold in HBMEC-associated, compared with HBMEC-unassociated, *M. tuberculosis* across the 5 data sets, using a δ-value of 1.33043 (median false discovery rate, 0).

Mutation of HBMEC-induced* M. tuberculosis *genes. Random insertion mutagenesis of *M. tuberculosis* CDC 1551 was performed in our laboratory using the *Himar1* transposon (Tn)

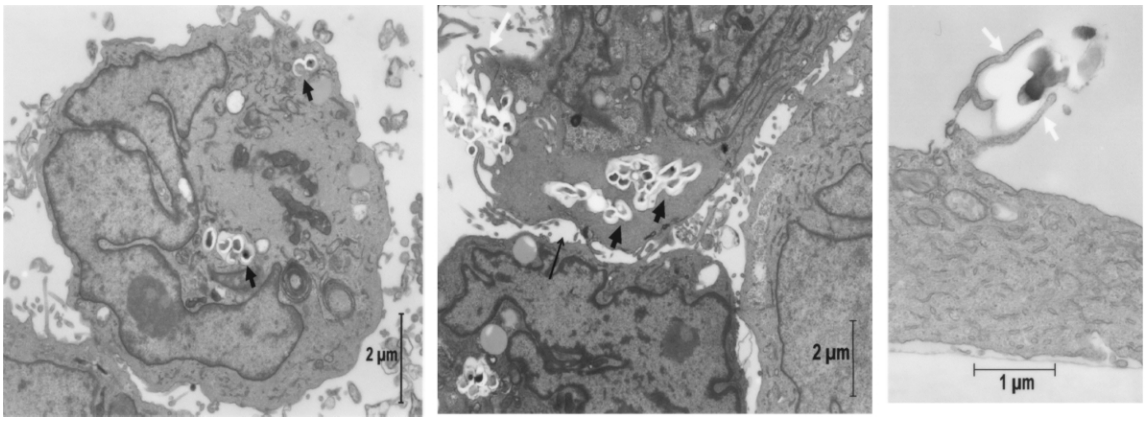

Figure 3. Cross-sectional *(left* and *middle)* and longitudinal *(right)* transmission electron micrographs of an infant human brain microvascular endothelial-cell (HBMEC) monolayer infected with *Mycobacterium tuberculosis* H37Rv. Electron-dense *(dark black) M. tuberculosis* is seen both intra- and extracellularly. Intracellular *M. tuberculosis* is seen inside endosomes *(thick black arrows).* Microvilli-like protrusions from HBMECs form around *M. tuberculosis (white arrows).* No *M. tuberculosis* is seen in the paracellular space *(thin black arrow).*

as part of a comprehensive insertional mutagenesis [28]. Tn insertion sites were identified by sequencing the insertion junction, as described elsewhere [29–31]. Relevant mutants available to us from our collection of *Himar1* Tn insertion mutants were used in the study. HBMEC invasion by mutants for 5 genes *(Rv0980c, Rv0987, Rv0989c, Rv0990c,* and *Rv1801),* which were up-regulated at least 8-fold in HBMEC-associated *M. tuberculosis* H37Rv (table 1), and for *Rv0981* were compared with that of an intergenic negative-control Tn mutant with Tn insertion at bp 921350, which falls between annotated genes *MT0849 (NT02MT0849)* and *MT0850 (Rv0829).* An invasion assay was performed as described above, except that streptomycin (200 μg/mL) was used instead of amikacin. This is because all the Tn mutants possess kanamycin cassettes that may interfere with amikacin killing [32].

Statistical analysis. All invasion, traversal, cytochalasin D inhibition, and mutant studies were performed at least in triplicate, and groups were compared statistically using the Mann-Whitney *U* test.

RESULTS

Invasion and traversal of the BBB model by mycobacteria. We tested whether *M. tuberculosis* was capable of invasion and traversal of our in vitro BBB model. We used *M. smegmatis,* a nonpathogenic mycobacterial species, as a negative control in our experiments. In addition, we tested *M. bovis* BCG and compared its invasion and traversal with those of *M. tuberculosis* laboratory strains H37Rv and CDC 1551. *M. tuberculosis* did not cause any noticeable lysis or detachment of the monolayer at the end of the invasion and traversal assays.

Invasion. *M. tuberculosis* H37Rv and CDC 1551 were found to invade HBMECs at a median invasion fraction of 2.6% (range, 1.0%–4.2%) and 2.7% (range, 0.8%–4.5%), respectively. The median invasion fraction for *M. smegmatis* was 0.18% (range, 0.0%–0.9%), which was significantly lower than that of *M. tuberculosis* CDC 1551 or H37Rv ($P < .0008$) (figure 2). The median invasion fraction for *M. bovis* BCG was 0.9% (range, 0.1%–2.8%), which was not significantly different from that for *M. tuberculosis* ($P = .07$).

Traversal. *M. tuberculosis* H37Rv and CDC 1551 were found to traverse HBMECs at a median traversal fraction of 3.4×10^{-4}% (range, 0.0–8.1×10^{-4}%) and 0.6×10^{-4}% (range, 0.2–1.1×10^{-4}%), respectively (figure 2). *M. smegmatis* was unable to traverse the HBMEC monolayer (lower limit of detection, 5.1×10^{-7}%; $P < .01$). The median traversal fraction for *M. bovis* BCG was 14.2×10^{-4}% (range, 10.0–18.3×10^{-4}%) and was not significantly different from that for *M. tuberculosis* ($P = .06$).

Transmission electron micrographs. On interaction with *M. tuberculosis,* HBMECs formed microvilli-like protrusions that surrounded and endocytosed mycobacteria (figure 3). This finding suggested that *M. tuberculosis* invasion and traversal requires actin cytoskeleton rearrangements in HBMECs. We therefore tested this hypothesis by performing colocalization and inhibition studies.

M. tuberculosis *invasion and HBMEC actin cytoskeleton rearrangements.* GFP-expressing *M. tuberculosis* (green) were found to colocalize with fluorescent phalloidin-stained actin at the surface of HBMECs (figure 4*A*–4*F*) consistently across several fields visualized by confocal microscopy. Treatment of HBMECs with cytochalasin D (an actin polymerization inhibitor) at 0.05 and 0.25 μg/mL did not alter the monolayer integrity; however, it significantly decreased the invasion by *M. tuberculosis,* compared with untreated HBMEC, by 61.0% and 76.7%, respectively ($P = .048$) (figure 4*G*).

M. tuberculosis *genes involved with invasion and intracellular survival in HBMECs.* We identified 180 *M. tuber-*

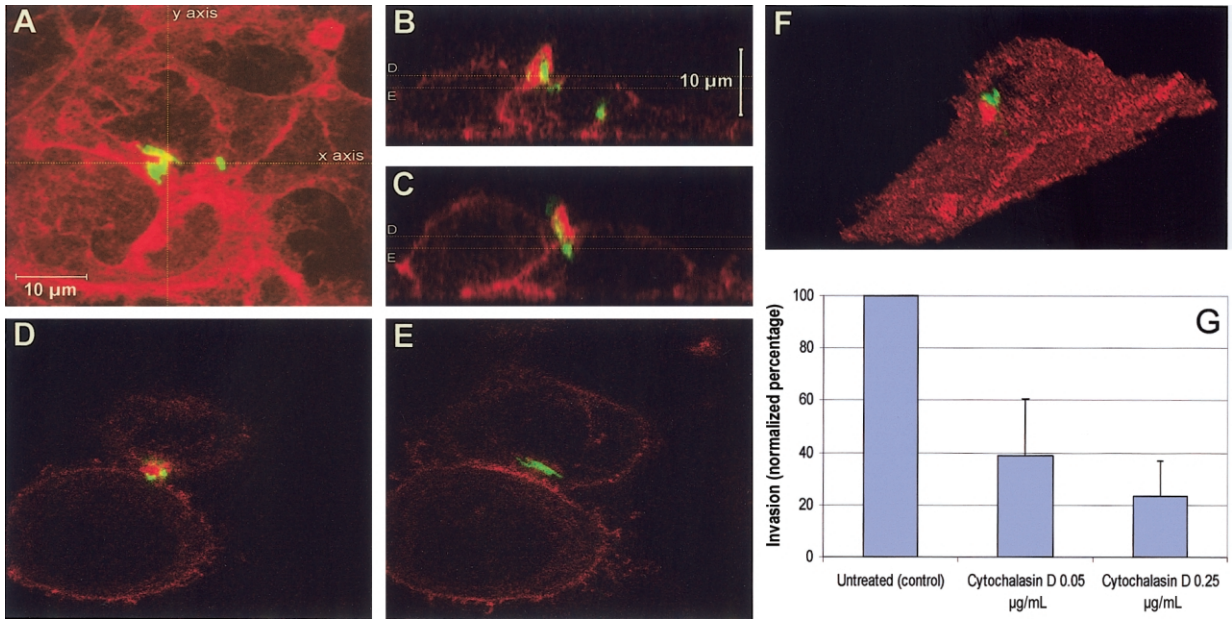

Figure 4. Actin colocalization with green fluorescent protein (GFP) expressing *Mycobacterium tuberculosis* in the infant human brain microvascular endothelial-cell (HBMEC) monolayer. HBMECs infected with GFP expressing *M. tuberculosis* were stained with red fluorescent phalloidin and visualized using a confocal microscope. *A, M. tuberculosis (green)* can be seen in a background of actin-stained HBMECs *(red). B* and *C,* Z section through the *X* and *Y* axes, respectively, showing actin colocalization with *M. tuberculosis. D* and *E,* XY sections (positions indicated in panels B and C) showing actin colocalization and intracellular *M. tuberculosis. F,* Three-dimensional rendering of HBMECs with GFP expressing *M. tuberculosis. G,* Significantly decreased invasion by *M. tuberculosis* H37Rv in HBMECs treated with cytochalasin D (actin polymerization inhibitor) at 0.05 and 0.25 μg/mL, compared with untreated HBMECs ($P = .048$).

culosis genes that were differentially regulated by at least 8-fold in HBMEC-associated, compared with HBMEC-unassociated, *M. tuberculosis.* The 33 up-regulated genes, with their annotated functions [33], are listed in table 1. The 147 down-regulated genes, with their annotated functions, are listed in table 2.

Mutation of HBMEC-induced* M. tuberculosis *genes and reduced HBMEC invasion. To determine whether genes up-regulated in response to contact with HBMECs also play a role in endothelial-cell invasion, we obtained *M. tuberculosis* CDC 1551 mutants in which genes were interrupted by Tn insertions. Invasion by mutants *Rv0980c, Rv0987, Rv0989c,* and *Rv1801* was significantly decreased, by 50.0% ($P = .0022$), 44.2% ($P = .0022$), 27.4% ($P = .0043$), and 66.1% ($P = .0022$), respectively, compared with the negative-control Tn mutant (figure 5). It should be noted that the *Rv0987* mutant used in our experiments has a Δ*sigF* background that could potentially have confounded our results [34]. We therefore compared HBMEC invasion by the *Rv0987* mutant with that of *M. tuberculosis* CDC 1551 Δ*sigF* and found that invasion by the *Rv0987* mutant was significantly decreased, by 34.3% ($P = .0022$), compared with *M. tuberculosis* CDC 1551 Δ*sigF.* These results indicate that genes *Rv0980c, Rv0987, Rv0989c,* and *Rv1801* are potentially required for endothelial-cell invasion and/or intracellular survival.

DISCUSSION

To produce CNS tuberculosis, *M. tuberculosis* needs to traverse the BBB formed by the specialized endothelial cells lining the brain microvasculature. Using HBMECs, we have been able to detect endothelial invasion and traversal by pathogenic mycobacteria. Unlike macrophages, endothelial cells are nonprofessional phagocytic cells, and they do not engulf extracellular material nonspecifically [35]. This is highlighted by the inability of HBMECs to take up naive carboxylated fluorescent 1-μm beads [36]. Nevertheless, *M. tuberculosis* was found to invade and traverse the HBMEC monolayers, which suggests that *M. tuberculosis* triggers its own uptake by HBMECs. In addition, we found that pathogenic *M. tuberculosis* strains H37Rv and CDC 1551 invade and traverse HBMEC monolayers more than the nonpathogenic species *(M. smegmatis),* which suggests that traversal by *M. tuberculosis* across the BBB (and, possibly, other cellular barriers) may be a specific process that requires particular virulence factors. At a cellular level, differences in invasion and traversal by *M. tuberculosis* and *M. smegmatis* may be explained either at the level of uptake or by initial intracellular survival in HBMECs [37, 38]. Further studies are under way to characterize this process. We observed that invasion and traversal by *M. bovis* BCG was similar to that of *M. tuberculosis.*

Table 2. Genes down-regulated by at least 8-fold in human brain microvascular endothelial-cell–associated vs. –unassociated *Mycobacterium tuberculosis* H37Rv.

The table is available in its entirety in the online edition of the *Journal of Infectious Diseases.*

This is consistent with the observation that the relative avirulence of BCG is not due to its inability to invade but, rather, to an inability to survive host immune-control mechanisms [39]. Traversal across the BBB requires the additional steps of prolonged intracellular survival and exocytosis from the other (brain) side of the cellular barrier. This is consistent with the much lower traversal rates (vs. invasion) observed by us for all mycobacteria tested—an observation that other researchers have seen in related model studies [18].

M. tuberculosis did not cause any noticeable lysis or detachment of the monolayer at the end of the invasion and traversal assays. Furthermore, electron microscopy of infected HBMECs suggested that *M. tuberculosis* invasion and traversal required actin cytoskeleton rearrangements by HBMECs. We tested this hypothesis and found that *M. tuberculosis* colocalized with surface actin of HBMECs and that treatment of HBMECs by cytochalasin D significantly decreased invasion by *M. tuberculosis.* These data suggest that traversal across the BBB might possibly be transcellular. However, concurrent pathogen-triggered paracellular traversal cannot be ruled out. Actin cytoskeleton rearrangements by HBMECs have been shown to be a prerequisite for invasion by several other meningitis-causing organisms via different signaling mechanisms [21]. Furthermore, Menozzi et al. [40] have shown that a 28-kDa *M. tuberculosis* adhesin protein induces actin cytoskeleton rearrangements in confluent bovine brain capillary endothelial cells and that it does not open the tight junctions of the endothelial monolayer. Our study, however, did not identify this gene to be differentially regulated in HBMEC-associated *M. tuberculosis* infection.

We hypothesized that genes significantly up-regulated in HBMEC-associated, compared with HBMEC-unassociated, *M. tuberculosis* are likely to be involved in HBMEC invasion and intracellular survival. Indeed, by *M. tuberculosis* whole-genome microarrays, we identified 33 genes that were up-regulated by at least 8-fold in HBMEC-associated *M. tuberculosis.* Talaat et al. [41] described an in vivo–expressed genomic island (iVEGI), *Rv0960–Rv1001,* that contains 20 *M. tuberculosis* genes that are up-regulated in mouse lungs, compared with in vitro growth. The majority of iVEGI genes are involved in cell-wall biosynthesis and lipid metabolism, and iVEGI genes are present in pathogenic mycobacteria *(M. tuberculosis* H37Rv and CDC 1551 and *M. bovis)* but not in *M. smegmatis.* Of the 33 genes identified by us, 18 belong to the same iVEGI, which suggests their potential role in virulence. Furthermore, 25 of 33 genes identified by us are predicted to be nonessential for in vitro growth, which suggests a potential role in in vivo survival and/or virulence.

To determine whether these 33 up-regulated genes also play a role in endothelial-cell invasion, we compared the invasion of their Tn mutants with that of a negative control mutant and found that the invasion by Tn mutants for *Rv0980c, Rv0987, Rv0989c,* and *Rv1801* was significantly decreased. However, the phenotypes displayed by these Tn mutants are relatively modest. This could be explained by partial inactivation of the gene

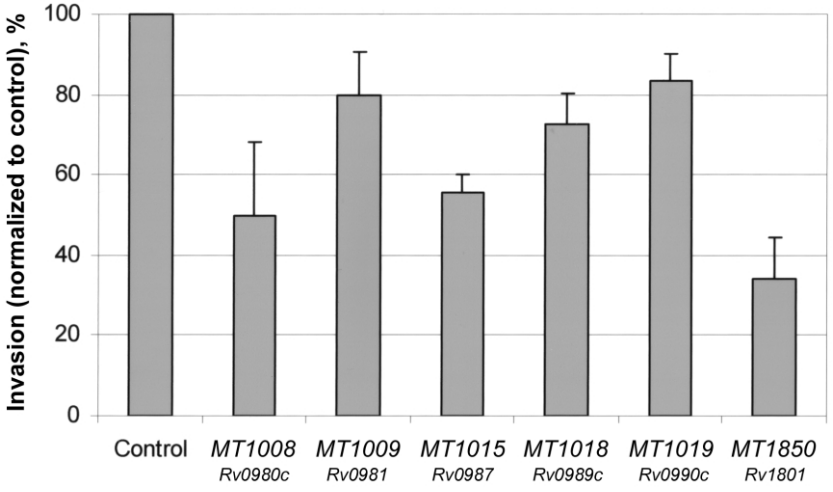

Figure 5. Invasion of the infant human brain microvascular endothelial-cell (HBMEC) monolayer by isogenic *Mycobacterium tuberculosis* mutants (normalized to control). Invasion of HBMECs by isogenic *M. tuberculosis* CDC 1551 Tn mutants *MT1008 (Rv0980c), MT1015 (Rv0987), MT1018 (Rv0989c),* and *MT1850 (Rv1801)* was significantly decreased, compared with the control mutant ($P < .0043$). The control mutant has an intergenic Tn insertion that falls between annotated genes *MT0849 (NT02MT0849)* and *MT0850 (Rv0829).* Medians are shown; the error bar represents the third quartile. Groups were compared statistically using the Mann-Whitney *U* test.

by the Tn insertion or by compensation through complementary pathways. In addition, although we believe that these genes are potentially required for endothelial-cell invasion and/or intracellular survival, a polar effect of the Tn insertion on downstream genes may be a possible confounding source. In vitro growth differences among the Tn mutants could also potentially confound our results; however, there were no significant differences in the in vitro growth or colony morphology for the mutants tested in the study. *Rv0980c, Rv0987,* and *Rv0989c* belong to the iVEGI described by Talaat et al. *Rv0987* belongs to an unclassified ATP binding cassette (ABC) transporter system and is postulated to function along with *Rv0986 (Rv0986* and *Rv0987* were both highly up-regulated in HBMEC-associated *M. tuberculosis).* The proteins encoded by *Rv0986* and *Rv0987* are homologous to the AttE-G proteins of *Agrobacterium tumefaciens,* which form an ABC transporter in *A. tumefaciens* and are involved in virulence and bacterial attachment to host cells [42, 43]. Therefore, protein products of *Rv0986* and *Rv0987* are thought to be involved in *M. tuberculosis* adhesion and virulence. An *Rv0986* Tn mutant has been shown to have decreased survival in macrophages, which supports its possible role in virulence [44]. Incidentally, *Rv0986–Rv0987* displays only a weak similarity to any ORF in *M. smegmatis* (*E* value, <0.05) [41]. Although HBMEC invasion by Tn mutants for *Rv0981* and *Rv0990c* was not significantly decreased, the Tn insertions in these genes were close to their distal ends (nt 547/693 and 612/656, respectively) and possibly cause partial gene inactivation.

The 147 genes that were down-regulated by at least 8-fold in HBMEC-associated *M. tuberculosis* H37Rv cluster in functional groups of transcription, protein synthesis, energy metabolism, and other metabolic pathways, which suggests that *M. tuberculosis* decreases its overall metabolic state very early during infection and internalization by endothelial cells. This relative shutdown of the active metabolism may be a precursor of latency, as has been postulated to occur in endothelial cells in human autopsy samples [20].

Schnappinger et al. [45] identified 601 *M. tuberculosis* genes that are significantly differentially regulated at 24 or 48 h after infection in either naive or interferon-γ–stimulated wild-type macrophages, using a false-discovery rate of <1%. Four of 454 induced genes *(galTb, PPE29, mce3C,* and *Rv3833)* and 37 of 147 repressed genes described by Schnappinger et al. are common to our 33 up-regulated and 147 down-regulated genes, respectively. Although different host cells were studied, it is also likely that experimental differences account for the relative lack of overlap in the patterns of bacterial gene expression between the present study and that of Schnappinger et al. For example, we studied gene expression at 2 h, compared with the 24 or 48 h in the Schnappinger et al. model. In addition, we identified genes that were at least 8-fold up-regulated (with a false discovery rate of 0%), compared with no fold cutoff in the Schnappinger et al. model. Some differences in gene-expression patterns may be related to an intrinsically different microenvironment in primary brain microvascular endothelial cells, which are nonprofessional phagocytic cells and, therefore, are unlike macrophages.

In summary, we have studied the interaction between *M. tuberculosis* and HBMECs and demonstrated both invasion and traversal of HBMEC monolayers by virulent mycobacteria. This in vitro system was based on the well-established role of HBMECs in the physiologic BBB protecting the CNS. Therefore, the model system may prove to be valuable in identifying mechanisms of *M. tuberculosis* entry into the CNS and the pathogenesis of tuberculous meningitis. Indeed, we identified 33 *M. tuberculosis* genes that are up-regulated during bacterial association with HBMECs, and mutants in 4 of these genes showed reduced HBMEC invasion. Further studies are under way to characterize the host-cell molecular pathways that are involved in HBMEC invasion by *M. tuberculosis* and the specific mechanisms by which the mutants identified in the study lack invasion and/or intracellular survival.

Acknowledgments

We thank Moises Hernandez and Qi-Jian Cheng (Johns Hopkins University, Baltimore, MD), for providing some of the transposon mutants used in the study; and Michael Zilliox (Johns Hopkins University, Baltimore, MD), for help with data analysis.

References

1. Kochi A. The global tuberculosis situation and the new control strategy of the World Health Organization. Bull World Health Organ **2001**; 79: 71–5.
2. Lincoln EM, Sordillo VR, Davies PA. Tuberculous meningitis in children: a review of 167 untreated and 74 treated patients with special reference to early diagnosis. J Pediatr **1960**; 57:807–23.
3. Jacobs RF, Starke JR. *Mycobacterium tuberculosis.* In: Long SS, Pickering LK, Prober CG, eds. Principles and practice of pediatric infectious diseases. 2nd ed. New York: Churchill Livingstone, **2003**:796–8.
4. Girgis NI, Sultan Y, Farid Z, et al. Tuberculosis meningitis, Abbassia Fever Hospital-Naval Medical Research Unit No. 3-Cairo, Egypt, from 1976 to 1996. Am J Trop Med Hyg **1998**; 58:28–34.
5. Hosoglu S, Geyik MF, Balik I, et al. Predictors of outcome in patients with tuberculous meningitis. Int J Tuberc Lung Dis **2002**; 6:64–70.
6. Thwaites GE, Hien TT. Tuberculous meningitis: many questions, too few answers. Lancet Neurol **2005**; 4:160–70.
7. Rubin LL, Staddon JM. The cell biology of the blood-brain barrier. Annu Rev Neurosci **1999**; 22:11–28.
8. Armand-DeLille PF. Role des poisons du bacille de Koch dans la meningite tuberculeuse et la tuberculose des centres nerveux: etude experimentale et anatomo-pathologique. Paris: Universite de Paris, **1903**: 187.
9. Rich AR, McCordock HA. The pathogenesis of tuberculous meningitis. Bull Johns Hopkins Hosp **1933**; 52:5–37.
10. Rich AR, McCordock HA. An enquiry concerning the role of allergy, immunity and other factors of importance in the pathogenesis of human tuberculosis. Bull Johns Hopkins Hosp **1929**; 44:273–382.
11. Drevets DA, Leenen PJ, Greenfield RA. Invasion of the central nervous system by intracellular bacteria. Clin Microbiol Rev **2004**; 17:323–47.

12. Lemierre A, Ameuille P. Granulie consécutive a l'injection intraveineuse volonteire d'une émulsion de bacilles de Koch. Bull Mem Soc Med Hop Paris **1938**; 54:286–95.
13. MacGregor AR, Green CA. Tuberculosis of the central nervous system, with special reference to tuberculous meningitis. J Pathol Bacteriol **1937**; 45:613–45.
14. Donald PR, Schaaf HS, Schoeman JF. Tuberculous meningitis and miliary tuberculosis: the Rich focus revisited. J Infect **2005**; 50:193–5.
15. Ransohoff RM, Kivisakk P, Kidd G. Three or more routes for leukocyte migration into the central nervous system. Nat Rev Immunol **2003**; 3: 569–81.
16. Dietrich JB. The adhesion molecule ICAM-1 and its regulation in relation with the blood-brain barrier. J Neuroimmunol **2002**; 128:58–68.
17. Wu HS, Kolonoski P, Chang YY, Bermudez LE. Invasion of the brain and chronic central nervous system infection after systemic *Mycobacterium avium* complex infection in mice. Infect Immun **2000**; 68: 2979–84.
18. Bermudez LE, Sangari FJ, Kolonoski P, Petrofsky M, Goodman J. The efficiency of the translocation of *Mycobacterium tuberculosis* across a bilayer of epithelial and endothelial cells as a model of the alveolar wall is a consequence of transport within mononuclear phagocytes and invasion of alveolar epithelial cells. Infect Immun **2002**; 70:140–6.
19. Birkness KA, Deslauriers M, Bartlett JH, White EH, King CH, Quinn FD. An in vitro tissue culture bilayer model to examine early events in *Mycobacterium tuberculosis* infection. Infect Immun **1999**; 67:653–8.
20. Hernandez-Pando R, Jeyanathan M, Mengistu G, et al. Persistence of DNA from *Mycobacterium tuberculosis* in superficially normal lung tissue during latent infection. Lancet **2000**; 356:2133–8.
21. Kim KS. Pathogenesis of bacterial meningitis: from bacteraemia to neuronal injury. Nat Rev Neurosci **2003**; 4:376–85.
22. Stins MF, Gilles F, Kim KS. Selective expression of adhesion molecules on human brain microvascular endothelial cells. J Neuroimmunol **1997**; 76:81–90.
23. Stins MF, Badger J, Kim KS. Bacterial invasion and transcytosis in transfected human brain microvascular endothelial cells. Microb Pathog **2001**; 30:19–28.
24. Stins MF, Shen Y, Huang SH, Gilles F, Kalra VK, Kim KS. Gp120 activates children's brain endothelial cells via CD4. J Neurovirol **2001**; 7:125–34.
25. Jacobsson S. Neurobiological effects of cannabinoid receptors. Available at: http://www.umu.se/pharm-neuro/pharmacology/forskning/BBB.html. Accessed 10 July 2005.
26. Mangan J, Monahan I, Butcher P. Gene expression during host-pathogen interactions: approaches to bacterial mRNA extraction and labelling for microarray analysis. In: Wren B, Dorrell N, eds. Functional microbial genomics. Vol. 33. Burlington, MA: Elsevier, **2002**:137–51.
27. Larsen M. Some common methods in mycobacterial genetics. In: Hatfull G, ed. Molecular genetics of *Mycobacteria.* Washington, DC: ASM Press, **2000**:317.
28. Tuberculosis Animal Research and Gene Evaluation Taskforce. Introgenic transposon mutants. Available at: http://www.hopkinsmedicine .org/TARGET/Studies.htm. Accessed 10 July 2005.
29. Rubin EJ, Akerley BJ, Novik VN, Lampe DJ, Husson RN, Mekalanos JJ. In vivo transposition of mariner-based elements in enteric bacteria and mycobacteria. Proc Natl Acad Sci USA **1999**; 96:1645–50.
30. Lamichhane G, Zignol M, Blades NJ, et al. A postgenomic method for predicting essential genes at subsaturation levels of mutagenesis: application to *Mycobacterium tuberculosis.* Proc Natl Acad Sci USA **2003**; 100: 7213–8.
31. Lamichhane G, Tyagi S, Bishai WR. Designer arrays for defined mutant analysis to detect genes essential for survival of *Mycobacterium tuberculosis* in mouse lungs. Infect Immun **2005**; 73:2533–40.
32. Kruuner A, Jureen P, Levina K, Ghebremichael S, Hoffner S. Discordant resistance to kanamycin and amikacin in drug-resistant *Mycobacterium tuberculosis.* Antimicrob Agents Chemother **2003**; 47:2971–3.
33. Cole S. Tuberculist. Data release R6, WWW server v3.1. Available at: http://genolist.pasteur.fr/Tuberculist. Accessed 11 November 2005.
34. Chen P, Ruiz RE, Li Q, Silver RF, Bishai WR. Construction and characterization of a *Mycobacterium tuberculosis* mutant lacking the alternate sigma factor gene, *sigF.* Infect Immun **2000**; 68:5575–80.
35. Sansonetti P. Host-pathogen interactions: the seduction of molecular cross talk. Gut **2002**; 50(Suppl 3):III2–8.
36. Kim KJ, Chung JW, Kim KS. 67-kDa laminin receptor promotes internalization of cytotoxic necrotizing factor 1-expressing *Escherichia coli* K1 into human brain microvascular endothelial cells. J Biol Chem **2005**; 280:1360–8.
37. Kim KJ, Elliott SJ, Di Cello F, Stins MF, Kim KS. The K1 capsule modulates trafficking of *E. coli*-containing vacuoles and enhances intracellular bacterial survival in human brain microvascular endothelial cells. Cell Microbiol **2003**; 5:245–52.
38. Russell DG. *Mycobacterium tuberculosis:* here today, and here tomorrow. Nat Rev Mol Cell Biol **2001**; 2:569–77.
39. Nuermberger EL, Yoshimatsu T, Tyagi S, Bishai WR, Grosset JH. Paucibacillary tuberculosis in mice after prior aerosol immunization with *Mycobacterium bovis* BCG. Infect Immun **2004**; 72:1065–71.
40. Menozzi FD, Reddy VM, Cayet D, et al. *Mycobacterium tuberculosis* heparin-binding haemagglutinin adhesin (HBHA) triggers receptor-mediated transcytosis without altering the integrity of tight junctions. Microbes Infect **2006**; 8:1–9.
41. Talaat AM, Lyons R, Howard ST, Johnston SA. The temporal expression profile of *Mycobacterium tuberculosis* infection in mice. Proc Natl Acad Sci USA **2004**; 101:4602–7.
42. Braibant M, Gilot P, Content J. The ATP binding cassette (ABC) transport systems of *Mycobacterium tuberculosis.* FEMS Microbiol Rev **2000**; 24:449–67.
43. Matthysse AG, Yarnall HA, Young N. Requirement for genes with homology to ABC transport systems for attachment and virulence of *Agrobacterium tumefaciens.* J Bacteriol **1996**; 178:5302–8.
44. Pethe K, Swenson DL, Alonso S, Anderson J, Wang C, Russell DG. Isolation of *Mycobacterium tuberculosis* mutants defective in the arrest of phagosome maturation. Proc Natl Acad Sci USA **2004**; 101:13642–7.
45. Schnappinger D, Ehrt S, Voskuil MI, et al. Transcriptional adaptation of *Mycobacterium tuberculosis* within macrophages: insights into the phagosomal environment. J Exp Med **2003**; 198:693–704.